Quantitative multiparametric MR analysis of small renal lesions: correlation with surgical pathology

Motoyo Yano,[1] Kathryn J. Fowler,[1] Santip Srisuwan,[2] Amber Salter,[3] Cary L. Siegel[1]

[1]Mallinckrodt Institute of Radiology, Washington University School of Medicine, 510 S. Kingshighway Blvd., Campus Box 8131, Saint Louis, MO 63110, USA
[2]Department of Radiology, Bangkok Hospital Chiang Mai, 88/8 Nong Pa Khrang, Muang Chiang Mai 50000, Thailand
[3]Division of Biostatistics, Washington University School of Medicine, 660 Euclid Ave., Campus Box 8067, St. Louis, MO 63110-1093, USA

Abstract

Purpose: The purpose of the study is to evaluate the utility of apparent diffusion coefficient (ADC), chemical shift signal intensity index (SII), and contrast enhancement in distinguishing between benign lesions and renal cell carcinoma (RCC) and between subtypes of renal lesions.
Methods: This retrospective study included 98 renal lesions (≤ 3 cm) on MRI with correlative surgical pathology. Scanner field strength, lesion location, and size were recorded. Two readers blinded to surgical pathology independently measured ADC ratio (ADC lesion/ADC non-lesion kidney), SII, and absolute/relative enhancement in the corticomedullary and nephrographic phases of contrast.
Results: There were 76 malignant and 22 benign lesions. 42 RCC were clear cell (ccRCC), 19 papillary (pRCC), 5 chromophobe (cbRCC). Benign lesions included both solid and cystic lesions. Interreader agreement for all variables was good–excellent (ICC 0.70–0.91). There was no difference in ADC or SII between benign and malignant lesions. There was greater absolute corticomedullary enhancement of benign versus malignant lesions (150.0 ± 111.5 vs. 81.1 ± 74.8, $p = 0.0115$), which did not persist when excluding pRCC. For lesion subtype differentiation, ADC_{ratio} for pRCC was lower than benign lesions (0.74 ± 0.35 vs. 1.03 ± 0.46, $p = 0.0246$). ccRCC demonstrated greater SII than other RCC (0.09 ± 0.22 vs. 0.001 ± 0.26, $p = 0.0412$). Oncocytomas and angiomyolipoma (AML) showed greater absolute corticomedullary enhancement than ccRCC and pRCC (145.6 ± 65.2 vs. 107.2 ± 85.3, $p = 0.043$ and 186.2 ± 93.9 vs. 37.6 ± 35.3, $p = 0.0108$), respectively.
Conclusions: While corticomedullary-phase enhancement was a differentiating feature, quantitative metrics from diffusion and chemical shift imaging cannot reliably differentiate benign from malignant lesions. Quantitative assessment may be useful in differentiating some benign and malignant lesion subtypes.

Key words: Renal mass—Magnetic resonance—Diffusion-weighted imaging—Enhancement—Chemical shift—Malignancy

The detection of small, asymptomatic renal lesions is increasing, related in part to increased utilization of cross-sectional imaging [1]. The risk of malignancy increases with the size of the renal lesion [2]. This in turn means that a significant number of small renal masses, typically defined as less than 4 cm in maximal diameter [3], are benign lesions. The difficulty in distinguishing between benign and malignant renal lesions, especially when lesions are small, is reflected in the benign outcome of some surgically resected renal lesions [2]. As there is potential for morbidity in the ablative or surgical management of small renal lesions [4], accurate radiologic assessment may improve patient outcomes.

The overlap in imaging appearance between benign and malignant renal lesions is in part related to the diverse histologic subtypes of renal cell carcinoma and the various benign histologic diagnoses which may manifest as a focal renal mass [5]. There are qualitative imaging features for some renal lesion subtypes which are gen-

Correspondence to: Motoyo Yano; *email:* myano@wustl.edu

erally well accepted and helpful in characterizing a renal mass. This includes T2 hypointensity and modest enhancement in papillary RCC (pRCC) [5]. Contrast hyperenhancement and intravoxel lipid is seen with clear cell RCC (ccRCC), the most common RCC subtype [5]. However, these same qualitative features may be observed with benign lesions such as angiomyolipomas (AML) and oncocytomas [6, 7].

MR imaging yields several distinct quantifiable features that may better differentiate renal masses than standard qualitative imaging assessment. Several authors have demonstrated that apparent diffusion coefficient (ADC) values measured on diffusion-weighted imaging are lower in solid malignant lesions than benign [8–11]. Likewise, studies regarding chemical shift suggest that quantitative analysis of signal intensity may be more robust in demonstrating differences between lesion subtypes than qualitative analysis [6]. Similar principles may apply to differences in contrast enhancement of benign versus malignant renal lesion subtypes [12, 13].

The goal of our study was to evaluate the utility of quantitative parameters derived from diffusion-weighted imaging, chemical shift imaging, and contrast enhancement, in distinguishing between benign lesions and renal cell carcinoma. Specific benign vs. malignant renal lesion subtype comparisons guided by established qualitative characteristics were performed for some parameters.

Materials and methods

Informed consent was waived by the institutional review board for this Heath Insurance Portability and Accountability Act-compliant retrospective study.

Study population

A surgical pathology database search for "renal mass" at our institution from January 2011 to September 2013 yielded 757 renal masses, of which 177 had pre-operative MRI (Fig. 1). Diffusion-weighted images or MR images were not available for 12 masses, yielding 165 masses. Additionally, 2 masses were excluded because no renal mass was seen, one was excluded for ESRD with pyelonephritis, and one case was excluded for pancreatic cancer enveloping the kidney. Additionally, 63 masses were excluded because lesion size was larger than 3 cm. No renal masses were excluded due to cystic appearance. This yielded a final population of 98 masses in 98 patients. Parameter-specific exclusions due to poor image quality from these 98 masses were as follows: ADC $n = 11$, corticomedullary phase $n = 8$, nephrographic phase $n = 2$, and chemical shift $n = 8$. In scenarios when multiple masses were present in the surgical specimen, only a single mass (largest under 3 cm and malignant) was included for each patient.
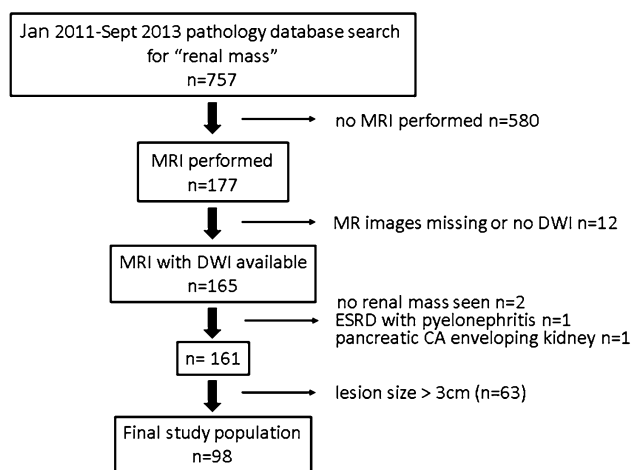
Fig. 1. Flow chart for study population. Parameter-specific exclusions for poor image quality from the final population of 98 included $n = 11$ for ADC, $n = 8$ for corticomedullary phase of enhancement, $n = 2$ for nephrographic phase of enhancement, and $n = 8$ for chemical shift imaging.

MR image acquisition

Abdominal MRI was performed on one of eleven 1.5T or two 3T Siemens scanners (Avanto, Symphony, Espree, Aera, Trio, Skyra) with a phased array body coil. The imaging protocol on the various scanners was similar and included diffusion-weighted imaging, free-breathing non-EKG gated, slice thickness 8–10 mm, with b values of 50, 400, and 800 s/mm^2. ADC maps generated by the scanner were utilized for measurement of ADC values. Axial and coronal pre- and post-contrast T1w fat-suppressed volumetric interpolated breath-held examination (VIBE) images were obtained using an approximate matrix size of 256 × 320, slice thickness of 3 mm, parallel imaging factor of two, and opposed-phase echo time, with a set scanner delay of 18 seconds, followed by three additional post-contrast phases to capture arteriographic, corticomedullary, and nephrographic phases. Dual echo chemical shift gradient recall T1w images were obtained at nominal in- and opposed-phase echo times with slice thickness of 6–8 mm, similar resolution to the VIBE sequence. Additionally, T2w half Fourier acquisition single-shot turbo spin echo and T2 Turbo spin echo with and without fat suppression images were also acquired though were not used for quantitative analysis.

Image analysis

Images were reviewed by an abdominal radiologist with over 20 years of abdominal imaging experience to identify the resected renal lesion by correlating data from pre- and post-operative imaging with operative summary and surgical pathology report. The laterality and size of the lesion, presence of cystic components, as well as the series

and image number on which the lesion was best seen was recorded. Two separate readers with 5 and 3 years of post-fellowship abdominal imaging experience, blinded to surgical pathology data, measured quantitative data for three parameters: ADC, signal intensity index (SII), and contrast enhancement (Fig. 2). The largest ellipsoid region of interest (ROI) was placed within the confines of the lesion to measure ADC_{mean}, in-phase signal intensity, opposed-phase signal intensity, precontrast signal intensity, corticomedullary-phase signal intensity, and nephrographic-phase signal intensity. ADC_{mean} of the ipsilateral non-lesion kidney (cortex and medulla) was measured by both readers. ADC_{mean} of the contralateral kidney was measured by a single reader (reader 2). Both readers also measured precontrast, corticomedullary, and nephrographic-phase enhancement of non-lesion ipsilateral cortex.

The following calculations were performed for each renal lesion:

$$ADC_{ratio} = (ADC_{mean}lesion)/(ADC_{mean}ipsilateral\ kidney)$$

$$Signal\ intensity\ index = (in\ phase - opposed\ phase)/in\ phase$$

Absolute corticomedullary enhancement
= (corticomedullary lesion) − (precontrast lesion)

Absolute nephrographic enhancement
= (nephrographic lesion) − (precontrast lesion)

Relative corticomedullary enhancement
= (corticomedullary lesion)
− (corticomedullary nonlesion cortex)

Relative nephrographic enhancement
= (nephrographic lesion)
− (nephrographic nonlesion cortex)

Absolute washout = (corticomedullary lesion)
− (nephrographic lesion)
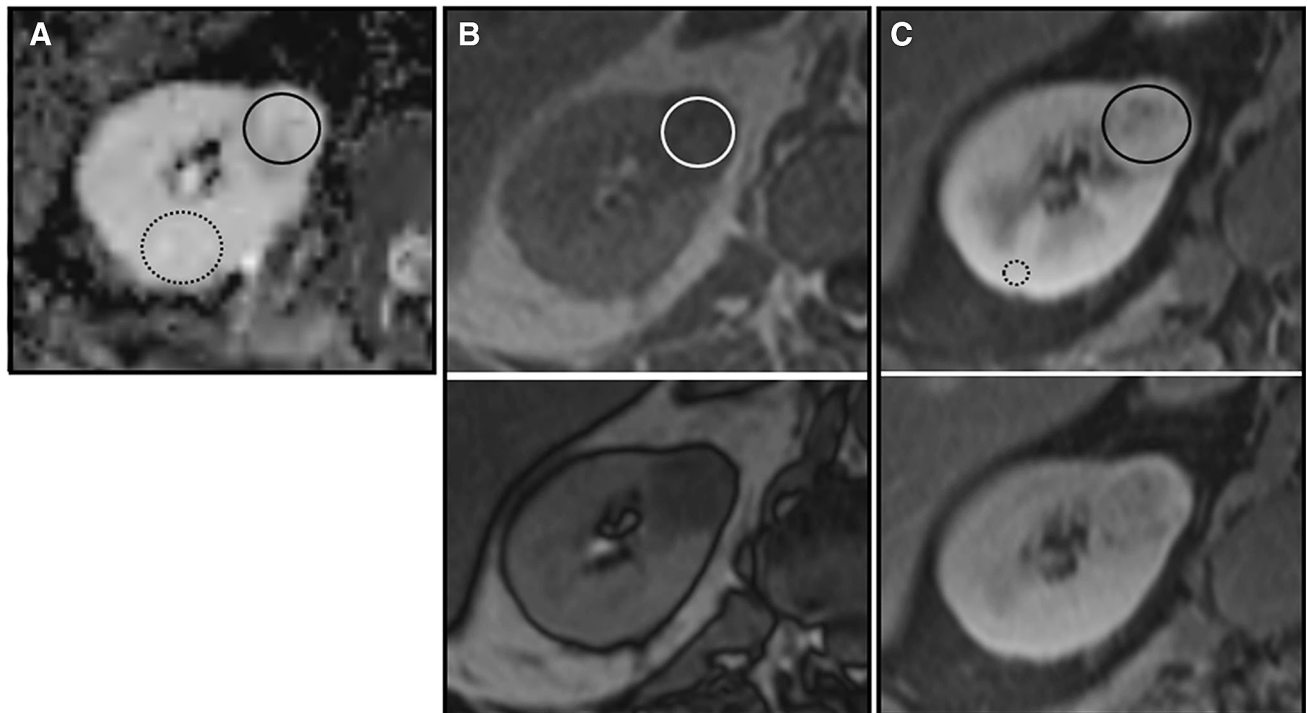
Fig. 2. A 60-year-old man with clear cell renal cell carcinoma in the right kidney. Quantitative parameter measurement technique is depicted. A The largest ellipsoid region of interest (ROI) was placed in the lesion (solid ellipse). The ADC of the non-tumor ipsilateral kidney, inclusive of cortex and medulla, was also measured on the same image whenever possible (dashed ellipse). B Similar ROI was placed within the lesion on in-phase (circle, top) and opposed-phase (bottom) images. C ROI was placed in the lesion on corticomedullary- (solid circle, top) and nephrographic (bottom)-phase images. Cortical enhancement in each phase of contrast was measured using an ROI placed in the cortex (dashed circle, top).

Statistical analysis

Descriptive statistics was used to summarize the data (mean (SD) and frequencies and percent). Interreader reliability was assessed using the intraclass correlation coefficient (ICC). ICC values of 0.5–0.75 were considered moderate agreement, 0.75–0.90 were considered good agreement, and greater than 0.90 were excellent agreement. Measures obtained from each reader were averaged after ensuring adequate agreement between the readers. Differences between benign and malignant renal lesions or between specific subtype comparisons were evaluated using t tests or Wilcoxon rank tests, as appropriate. Multivariable logistic regression with backward stepwise selection (stopping based on minimum Bayesian information criterion) was used to identify predictors of malignancy. The significance level was set at 0.05 for this study. Analyses were conducted in SAS v9.4.

Results

Lesion diagnosis by surgical pathology

Of the 98 total renal lesions, 76 lesions were malignant and 22 lesions were benign (Table 1). All of the malignant lesions were renal cell carcinomas, and the majority were clear cell RCC (ccRCC; $n = 42$) and papillary RCC (pRCC; $n = 19$). The benign lesions included 8

Table 1. Surgical pathology diagnoses of the 98 small renal masses

	n
Malignant	
Clear cell (cc)	42
Papillary (p)	19
Chromophobe (cb)	5
Other/unclassified	10
Total malignant	76
Benign	
Oncocytoma	8
Angiomyolipoma (AML)	6
Metanephric adenoma	2
Hemangioma	1
Chronic inflammation	1
Cysts	2
Leiomyoma	1
Pseudocyst	1
Total benign	22

oncocytomas and 6 angiomyolipomas (AML). Twelve renal lesions were predominantly cystic: 4 ccRCC, 3 pRCC, 2 cysts, 1 pseudocyst, 1 chronic inflammation, and 1 hemangioma.

Interobserver reliability

Interreader agreement was good for all quantitative measures assessed (Table 2) with ICC ranging from 0.709 to 0.912.
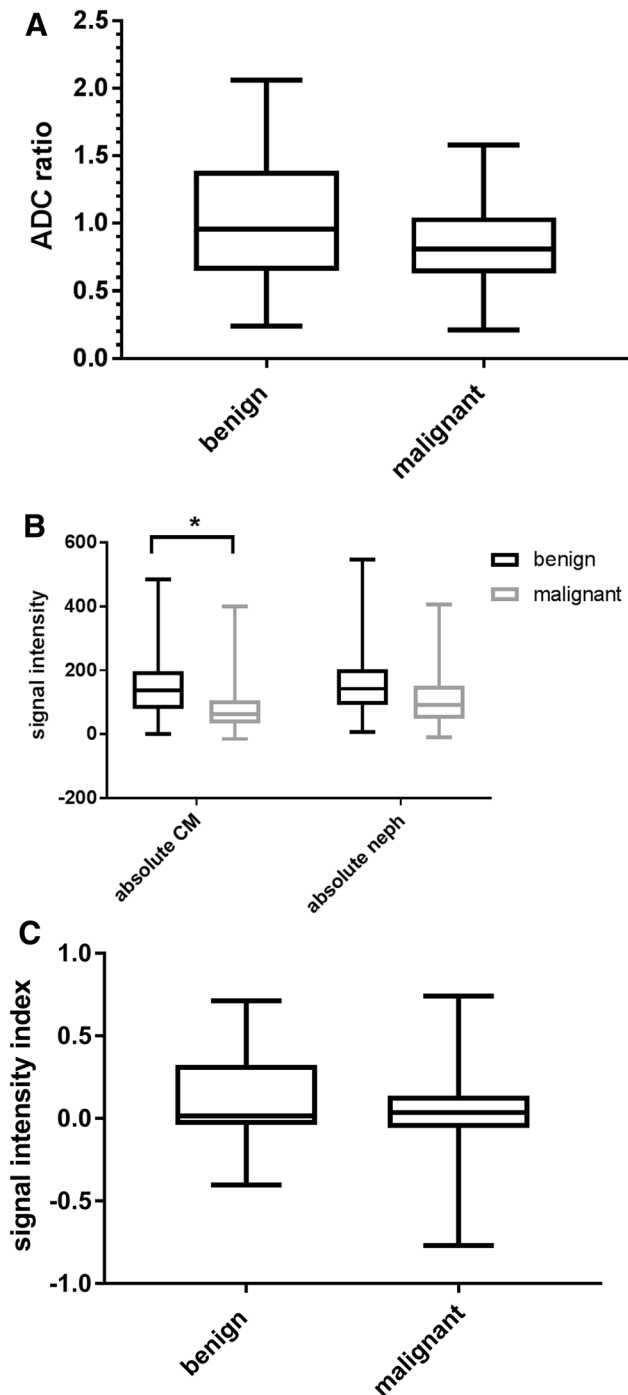
Benign versus malignant lesions

There was no significant difference in ADC_{ratio} between benign or malignant lesions (1.03 ± 0.456 vs. 0.85 ± 0.294, $p = 0.1130$, Fig. 3A). There were also no differences in SII between benign and malignant lesions (0.10 ± 0.27 vs. 0.05 ± 0.25, $p = 0.9468$, Fig. 3C). Benign lesions demonstrated significantly greater absolute corticomedullary enhancement compared to malignant lesions (150.02 ± 111.52 vs. 81.13 ± 74.81, $p = 0.0115$; Fig. 3B). This difference was no longer present when pRCC were excluded from the malignant lesions (150.02 ± 111.5 vs. 96.80 ± 79.21, $p = 0.0516$). No difference in absolute nephrographic enhancement, relative corticomedullary enhancement, relative nephrographic enhancement, or absolute washout was found between benign and malignant lesions (160.41 ± 119.55 vs. 110.83 ± 86.58, $p = 0.0812$, -142.93 ± 115.80 vs. -137.34 ± 123.44, $p = 0.8474$, -120.30 ± 112.72 vs. -113.55 ± 99.95, $p = 0.8021$, -10.39 ± 66.98 vs. -21.99 ± 37.29, $p = 0.4456$, respectively).

ADC_{mean} for the non-lesion ipsilateral kidney was significantly higher for malignant lesions compared to benign lesions ($2.17 \times 10^{-3} \pm 0.41 \times 10^{-3}$ vs. $1.95 \times 10^{-3} \pm 0.44 \times 10^{-3}$, $p = 0.0398$) and this was not dependent on scanner strength (not shown). ADC_{mean} for the contralateral kidney in patients with malignant lesions was also greater than patients with benign lesions ($2.19 \times 10^{-3} \pm 0.37 \times 10^{-3}$ vs. $1.95 \times 10^{-3} \pm 0.36 \times 10^{-3}$, $p = 0.011$). There was no significant difference in ADC_{mean} values between ipsilateral and contralateral kidneys when controlling for benign or malignant lesions (not shown).

Table 2. Interreader reliability

ADC	ICC	Chemical shift	ICC	Contrast enhancement	ICC
ADC_{mean} lesion	0.796	IP lesion	0.899	Absolute corticomedullary lesion	0.812
ADC_{mean} kidney	0.860	OP lesion	0.912	Absolute nephrographic lesion	0.822
ADC_{ratio}	0.772	SII	0.740	Relative corticomedullary lesion	0.786
				Relative nephrographic lesion	0.709
				Absolute lesion washout	0.705

IP, in-phase signal intensity; OP, opposed-phase signal intensity; SII, signal intensity index; ADC, apparent diffusion coefficient; ICC, intraclass correlation coefficient

A

B

C

◄Fig. 3. Box plots for quantitative multiparametric assessment of benign vs. malignant renal lesions. **A** There is no significant difference in ADC_{ratio} between benign and malignant renal lesions. **B** There is greater absolute corticomedullary enhancement of benign compared to malignant lesions, but this difference is not apparent for absolute nephrographic enhancement. No difference in relative corticomedullary or nephrographic enhancement was found for benign vs. malignant lesions (not shown). **C** For SII, no difference was found. Boxes represent the 25th and 75th percentile, with horizontal line within the box representing the median, and lines extending from the box indicating minimum and maximum values. Asterisk indicates a significant difference between groups flanked by bracket.

comedullary enhancement ($p = 0.013$) are retained as predictors of malignancy (AUC = 0.785).

Lesion subtype comparisons

ADC_{ratio}, absolute corticomedullary phase enhancement, and SII for benign and malignant renal lesion subtypes are shown in Fig. 4. Several significant differences are present in specific subtype comparisons for each parameter.

For ADC, pRCC shows a significantly lower ADC_{ratio} compared to benign lesions, but not compared to other RCC (0.74 ± 0.35 vs. 1.03 ± 0.46 vs. 0.89 ± 0.26, respectively, $p = 0.0246$; Fig. 5). No significant difference was found for similar analyses of ADC_{mean} (1.58 ± 0.81 vs. 1.92 ± 0.74 vs. 1.92 ± 0.60, $p = 0.1813$). For specific subtype comparisons (Table 3), there was no difference in ADC_{ratio} between oncocytoma and ccRCC, oncocytoma and cbRCC, or between AML and pRCC.

Absolute corticomedullary enhancement was greater for oncocytomas than ccRCC (Table 3). Oncocytomas demonstrated greater absolute nephrographic enhancement than cbRCC (194.4 ± 92.4 vs. 83.4 ± 92.4, $p = 0.049$) but no difference was found for absolute corticomedullary enhancement (Table 3). AML demonstrate greater enhancement than pRCC for both absolute corticomedullary enhancement (Table 3) and nephrographic enhancement (138.6 ± 51.6 vs. 60.8 ± 37.4, $p = 0.0117$). There was no difference in precontrast T1 signal intensity between ccRCC, cbRCC, pRCC, other RCC, and oncocytoma ($p = 0.818$).

For chemical shift imaging, there was a significant difference in SII between ccRCC and non-ccRCC subtypes (0.09 ± 0.22 vs. 0.001 ± 0.26, $p = 0.0412$; Fig. 6). There was no significant difference in SII between AML and ccRCC or between oncocytoma and ccRCC (Table 3).

To jointly examine the variables that best predict malignancy, ADC_{mean} lesion, ADC_{mean} kidney, ADC_{ratio}, in-phase signal intensity, opposed-phase signal intensity, SII, absolute corticomedullary enhancement, absolute nephrographic enhancement, relative corticomedullary enhancement, relative nephrographic enhancement, and absolute washout were entered into stepwise logistic regression analysis. In the final model, only ADC_{ratio} ($p = 0.042$) and absolute corti-

A

B

C
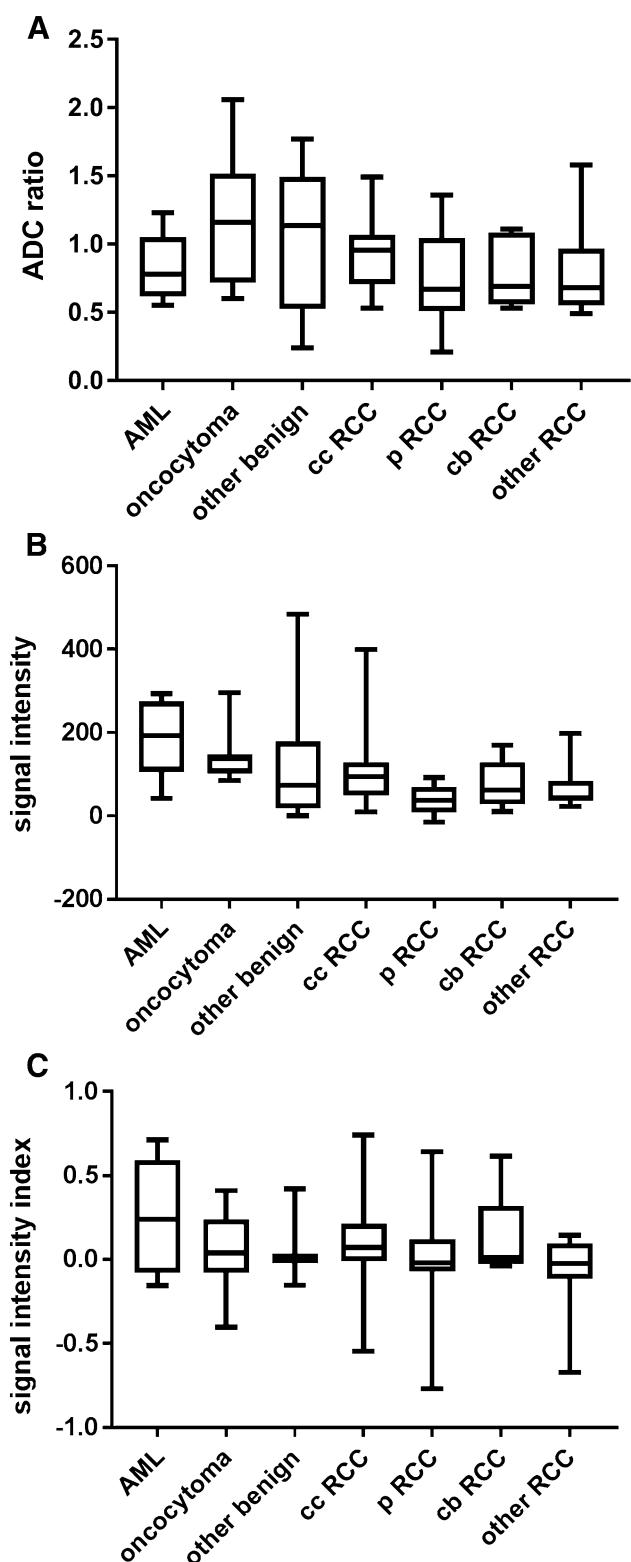
◄Fig. 4. Box plots showing quantitative multiparametric assessment of renal lesion subtypes. **A** ADC_{ratio}, **B** absolute corticomedullary-phase enhancement, and **C** signal intensity index are shown. Boxes represent the 25th and 75th percentile, with horizontal line within the box representing the median, and lines extending from the box indicating minimum and maximum values.
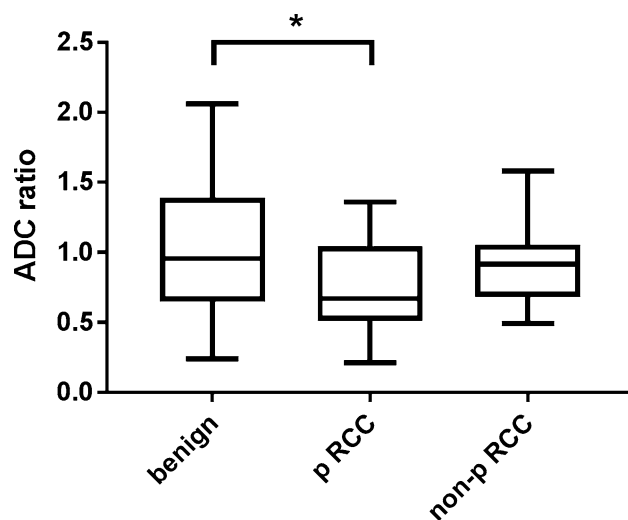

Fig. 5. Box plot comparison of ADC_{ratio} between pRCC, non-pRCC, and benign lesions. ADC ratio of pRCC is significantly lower than benign lesions, but not different than non-pRCC. Boxes represent the 25th and 75th percentile, with horizontal line within the box representing the median, and lines extending from the box indicating minimum and maximum values. Asterisk indicates a significant difference between groups flanked by bracket.

Discussion

Our study aimed to determine if quantitative data could be used to discriminate between benign and malignant renal lesions, and in this regard differs from many other studies which performed subtype-specific comparisons for specific MR parameters without a regard for lesion size. Our approach to focal renal lesions is potentially more reflective of clinical practice in which benign lesions need to be distinguished from malignant lesions. We found that ADC could not distinguish benign and malignant lesions, contrary to a prior report [8]. This is likely related to the greater diversity of benign lesions included in our study, including solid lesions such as oncocytoma and AML, and cystic appearing lesions such as chronic inflammation, hemangioma, cysts, and pseudocysts. SII was not helpful in distinguishing benign from malignant, as there are both malignant and benign lesions which demonstrate intravoxel lipid [6]. With regard to contrast enhancement, there was no difference in relative enhancement between benign and malignant lesions. However, absolute values calculated by subtract-

Table 3. Select comparisons for benign vs. malignant lesions

Benign lesion		Malignant lesion		p value
Mean	SD	Mean	SD	
ADC$_{ratio}$				
Oncocytoma ($n = 8$)		ccRCC ($n = 34$)		
1.19	0.496	0.93	0.236	0.2558[a]
Oncocytoma ($n = 8$)		cbRCC ($n = 5$)		
1.19	0.496	0.80	0.27	0.1896[a]
AML ($n = 6$)		pRCC ($n = 18$)		
0.83	0.251	0.74	0.35	0.5014
Absolute CM enhancement				
Oncocytoma ($n = 8$)		ccRCC ($n = 36$)		
145.6	65.2	107.2	85.3	0.0430
Oncocytoma ($n = 8$)		cbRCC ($n = 5$)		
145.6	65.2	75.4	60.0	0.0777
AML ($n = 6$)		pRCC ($n = 18$)		
186.2	93.9	37.6	35.3	0.0108
SII				
AML ($n = 6$)		ccRCC ($n = 36$)		
0.255	0.365	0.090	0.221	0.5774[a]
Oncocytoma ($n = 7$)		ccRCC ($n = 36$)		
0.039	0.254	0.090	0.221	0.5901[a]

Clinically relevant renal lesion subtype comparisons between benign and malignant lesions were performed for the three parameters
[a]Wilcoxon rank-sums test, median, and IQR are given
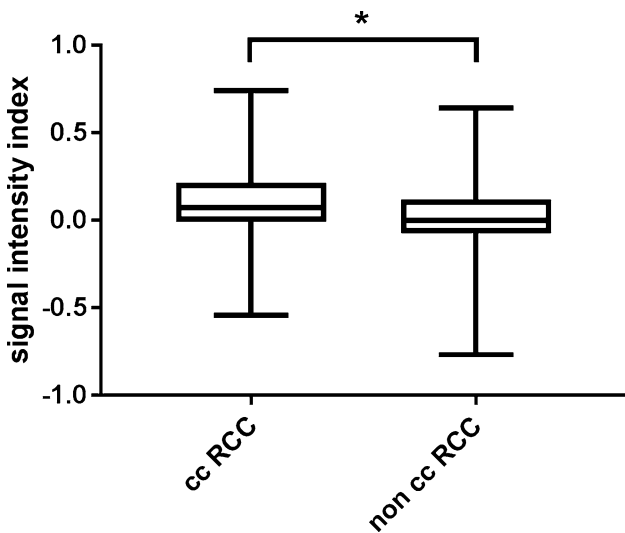
Fig. 6. Box plot comparison of ccRCC and non-ccRCC shows significantly higher SI index, or greater loss of signal on opposed-phase images, for ccRCC than other RCC. Boxes represent the 25th and 75th percentile, with horizontal line within the box representing the median, and lines extending from the box indicating minimum and maximum values. Asterisk indicates a significant difference between groups flanked by bracket.

ing precontrast lesion signal intensity from the corticomedullary phase, demonstrated differences. There was greater enhancement of benign lesions in the corticomedullary phase compared to malignant lesions, but this difference was no longer present when excluding pRCC from the malignant group, reflective of the well-

established hypoenhancing nature of pRCC [5, 14, 15]. Therefore, hyperenhancing benign and malignant lesions are not distinguishable. Of all the variables assessed in our three MR sequence parameters, stepwise logistic regression analysis shows that ADC$_{ratio}$ and absolute corticomedullary enhancement appear to be most helpful in distinguishing between benign and malignant lesions; this is supported by our subtype-specific comparisons as well.

Renal lesion subtype comparisons informed by qualitative MR features are more common in the literature. For example, oncocytomas and cbRCC have overlapping imaging appearance on MR [13] due to their common histologic classification as oncocytic neoplasms derived from intercalated cells of the collecting duct, and distinction on core needle biopsy is difficult [16]. Quantitatively, some authors have demonstrated greater ADC in oncocytomas than cbRCC [12, 17, 18], while others have not [14]. We did not find a difference in ADC$_{ratio}$ between oncocytoma and cbRCC. Contrary to other reports [12, 19, 20], we did not find a significant difference in contrast enhancement between oncocytoma and cbRCC.

When comparing oncocytomas to ccRCC, we found no difference in SII or ADC$_{ratio}$, but did find that oncocytomas demonstrate greater enhancement than ccRCC in the corticomedullary phase. The difference in enhancement is consistent with one report in the literature [21], but is discrepant compared to others who have found that ccRCC enhance greater than oncocytomas [22, 23] and others showing no difference in enhancement [7, 24, 25].

Conventional AML contain detectable bulk fat, allowing for their benign diagnosis, but minimal fat AML can have a T2 hypointense appearance similar to pRCC [26]. We found no difference in ADC between AML and pRCC, contrary to Park and Kim who found that minimal fat AML demonstrated greater ADC than pRCC (and other T2 hypointense RCCs) [27]. However, these lesions can be distinguished by their enhancement. We found that pRCC enhance less than AML, consistent with prior reports in the literature [26, 28–30].

We found that ADC$_{ratio}$ of pRCC was significantly lower than other renal lesions, consistent with the literature [9, 14, 17, 31–33]. In particular, we found that ADC$_{ratio}$ of pRCC was significantly lower than benign lesions. This finding is of interest in cases where lesion enhancement is difficult to ascertain, as the ADC$_{ratio}$ may aid in differentiating a benign-complicated cyst from a pRCC. However, since T1 hyperintense (hemorrhagic or proteinaceous) cysts can have lower ADC than T1 hypointense simple cysts [8], additional studies which include a large number of T1 hyperintense cysts will likely be necessary to confirm the utility of ADC in distinguishing between a hemorrhagic cyst and pRCC.

The SII of ccRCC is significantly greater than other RCC, consistent with prior reports [5, 6, 34, 35], and is reflective of the intracytoplasmic lipid within these lesions [5]. However, we found no difference in SII between ccRCC and benign lesions (AML and oncocytoma), which limits the utility of chemical shift imaging in distinguishing between malignant and benign lesions, and supports the notion that loss of signal on chemical shift imaging is not a specific feature of ccRCC [36].

There are several explanations for our paucity of discriminatory values in benign vs. malignant lesions compared to others. First, we limited our study population to lesions less than 3 cm in size, contrary to other studies evaluating ADC [8–11, 14, 17, 31, 32] or contrast enhancement [12, 14, 17, 19, 20], without limits on lesion size. Large lesions allow for the selective sampling of the most diffusion restricting portion of the lesion [8, 9, 31, 32] or assessment of enhancement in the portion of the lesion which meets a minimum threshold of enhancement [12, 14]. This approach is difficult to apply in the small lesions included in our study, and therefore, we assessed the entirety of the lesion (largest ellipsoid ROI which could fit in the lesion) for all parameters, potentially "diluting" our quantitative results compared to others. Second, the MR examinations included in our study were performed on one of eleven 1.5 T scanners and two 3 T scanners rather than single scanners [9, 14, 27, 31, 33, 37] or single field strength [11, 17, 32] used by others. There is likely variability in ADC values across scanners. For example, reported normal ADC values of kidneys range from 1.79×10^{-3} to 3.56×10^{-3} mm^2 s^{-1} [38–41]. While our population accurately reflects clinical practice in a large academic institution, single-scanner studies are potentially more robust because they are controlling for this variance.

As a measure to control for scanner variability, we normalized our tumor ADC values to the ipsilateral non-tumor kidney. Normalization in this manner resulted in significant differences between pRCC and benign lesions, otherwise not appreciated. This is driven in part by greater ADC$_{mean}$ values in non-tumor ipsilateral kidney of malignant lesions compared to benign lesions. Normalization of ADC is not novel [10, 12, 14, 18], but none have directly compared the ADC of the non-tumor kidney between benign and malignant lesions. This finding may perhaps be attributed to perfusion and flow phenomena in addition to Brownian motion of water molecules reflected in the monoexponential calculation of ADC from commercially available scanner output [42]. Combined with prior reports showing decreased renal ADC in acute renal failure, chronic renal failure, dehydration, ureteral obstruction, and renal artery stenosis [38, 41, 43], one can speculate that there may be increased perfusion to the kidneys in the presence of malignant lesions. Validation in larger data sets would be necessary, but if a difference in ADC$_{mean}$ of the back-

ground kidney of benign vs. malignant lesions can be redemonstrated independent of scanner type, this may be helpful in lesion characterization.

There are some limitations to this study. First, this was a retrospective study and this inherently leads to a selection bias. Second, our results reflect a variable pool of MR scanners and contrast agents. As previously discussed however, the heterogeneity of scanners may in fact be a strength of this study, challenging the applicability of previously reported single-scanner quantitative data in the clinical setting; if quantitative data are to be of clinical utility, it must be applicable across multiple scanner platforms. Third, we did not control for the Fuhrman grade of tumor, which has previously been shown to affect both ADC values [9] and the amount of intracellular lipid within ccRCC [44].

Conclusion

Despite good interreader reliability of quantitative MR parameters, no significant differences in ADC and SII could be demonstrated between benign and malignant lesions. There was greater corticomedullary phase enhancement of benign compared to malignant lesions. Future quantitative analyses to distinguish between benign and malignant small renal lesions on MR should focus on ADC$_{ratio}$ and corticomedullary-phase contrast enhancement.

References

1. Collins S, McKiernan J, Landman J (2006) Update on the epidemiology and biology of renal cortical neoplasms. J Endourol 20(12):975–985. https://doi.org/10.1089/end.2006.20.975
2. Johnson DC, Vukina J, Smith AB, et al. (2015) Preoperatively misclassified, surgically removed benign renal masses: a systematic review of surgical series and United States population level burden estimate. J Urol 193(1):30–35. https://doi.org/10.1016/j.juro.2014.07.102
3. Ha SC, Zlomke HA, Cost N, Wilson S (2015) The past, present, and future in management of small renal masses. J Oncol 2015:364807. https://doi.org/10.1155/2015/364807
4. Volpe A, Cadeddu JA, Cestari A, et al. (2011) Contemporary management of small renal masses. Eur Urol 60(3):501–515. https://doi.org/10.1016/j.eururo.2011.05.044

5. Pedrosa I, Sun MR, Spencer M, et al. (2008) MR imaging of renal masses: correlation with findings at surgery and pathologic analysis. Radiographics 28(4):985–1003. https://doi.org/10.1148/rg.2840 65018

6. Karlo CA, Donati OF, Burger IA, et al. (2013) MR imaging of renal cortical tumours: qualitative and quantitative chemical shift imaging parameters. Eur Radiol 23(6):1738–1744. https://doi.org/ 10.1007/s00330-012-2758-x

7. Pierorazio PM, Hyams ES, Tsai S, et al. (2013) Multiphasic enhancement patterns of small renal masses (≤4 cm) on preoperative computed tomography: utility for distinguishing subtypes of renal cell carcinoma, angiomyolipoma, and oncocytoma. Urology 81(6):1265–1271. https://doi.org/10.1016/j.urology.2012.12.049

8. Sandrasegaran K, Sundaram CP, Ramaswamy R, et al. (2010) Usefulness of diffusion-weighted imaging in the evaluation of renal masses. AJR Am J Roentgenol 194(2):438–445. https://doi.org/10. 2214/AJR.09.3024

9. Mirka H, Korcakova E, Kastner J, et al. (2015) Diffusion-weighted imaging using 3.0 T MRI as a possible biomarker of renal tumors. Anticancer Res 35(4):2351–2357

10. Erbay G, Koc Z, Karadeli E, et al. (2012) Evaluation of malignant and benign renal lesions using diffusion-weighted MRI with multiple b values. Acta Radiol 53(3):359–365. https://doi.org/10.1258/a r.2011.110601

11. Razek AA, Farouk A, Mousa A, Nabil N (2011) Role of diffusion-weighted magnetic resonance imaging in characterization of renal tumors. J Comput Assist Tomogr 35(3):332–336. https://doi.org/10. 1097/RCT.0b013e318219fe76

12. Galmiche C, Bernhard JC, Yacoub M, et al. (2017) Is multiparametric MRI useful for differentiating oncocytomas from chromophobe renal cell carcinomas? AJR Am J Roentgenol 208(2):343–350. https://doi.org/10.2214/AJR.16.16832

13. Rosenkrantz AB, Hindman N, Fitzgerald EF, et al. (2010) MRI features of renal oncocytoma and chromophobe renal cell carcinoma. AJR Am J Roentgenol 195(6):W421–427. https://doi.org/10. 2214/AJR.10.4718

14. Cornelis F, Tricaud E, Lasserre AS, et al. (2014) Routinely performed multiparametric magnetic resonance imaging helps to differentiate common subtypes of renal tumours. Eur Radiol 24(5):1068–1080. https://doi.org/10.1007/s00330-014-3107-z

15. Roy C, Sauer B, Lindner V, et al. (2007) MR Imaging of papillary renal neoplasms: potential application for characterization of small renal masses. Eur Radiol 17(1):193–200. https://doi.org/10.1007/s 00330-006-0271-9

16. Patel HD, Druskin SC, Rowe SP, et al. (2017) Surgical histopathology for suspected oncocytoma on renal mass biopsy: a systematic review and meta-analysis. BJU Int 119(5):661–666. h ttps://doi.org/10.1111/bju.13763

17. Taouli B, Thakur RK, Mannelli L, et al. (2009) Renal lesions: characterization with diffusion-weighted imaging versus contrast-enhanced MR imaging. Radiology 251(2):398–407. https://doi.org/ 10.1148/radiol.2512080880

18. Zhong Y, Wang H, Shen Y, et al. (2017) Diffusion-weighted imaging versus contrast-enhanced MR imaging for the differentiation of renal oncocytomas and chromophobe renal cell carcinomas. Eur Radiol. https://doi.org/10.1007/s00330-017-4906-9

19. Dhyani M, Grajo JR, Rodriguez D, et al. (2017) Aorta-Lesion-Attenuation-Difference (ALAD) on contrast-enhanced CT: a potential imaging biomarker for differentiating malignant from benign oncocytic neoplasms. Abdom Radiol (NY) 42(6):1734–1743. https://doi.org/10.1007/s00261-017-1061-3

20. Choi JH, Kim JW, Lee JY, et al. (2015) Comparison of computed tomography findings between renal oncocytomas and chromophobe renal cell carcinomas. Korean J Urol 56(10):695–702. http s://doi.org/10.4111/kju.2015.56.10.695

21. Bird VG, Kanagarajah P, Morillo G, et al. (2011) Differentiation of oncocytoma and renal cell carcinoma in small renal masses (< 4 cm): the role of 4-phase computerized tomography. World J Urol 29(6):787–792. https://doi.org/10.1007/s00345-010-0586-7

22. Jinzaki M, Tanimoto A, Mukai M, et al. (2000) Double-phase helical CT of small renal parenchymal neoplasms: correlation with pathologic findings and tumor angiogenesis. J Comput Assist Tomogr 24(6):835–842

23. Young JR, Margolis D, Sauk S, et al. (2013) Clear cell renal cell carcinoma: discrimination from other renal cell carcinoma subtypes and oncocytoma at multiphasic multidetector CT. Radiology 267(2):444–453. https://doi.org/10.1148/radiol.13112617

24. Chen F, Gulati M, Hwang D, et al. (2017) Voxel-based whole-lesion enhancement parameters: a study of its clinical value in differentiating clear cell renal cell carcinoma from renal oncocytoma. Abdom Radiol (NY) 42(2):552–560. https://doi.org/10.1007/ s00261-016-0891-8

25. Lee-Felker SA, Felker ER, Tan N, et al. (2014) Qualitative and quantitative MDCT features for differentiating clear cell renal cell carcinoma from other solid renal cortical masses. AJR Am J Roentgenol 203(5):W516–524. https://doi.org/10.2214/AJR.14.124 60

26. Lim RS, Flood TA, McInnes MDF, Lavallee LT, Schieda N (2017) Renal angiomyolipoma without visible fat: can we make the diagnosis using CT and MRI? Eur Radiol. https://doi.org/10.1007/s00 330-017-4988-4

27. Park JJ, Kim CK (2017) Small (< 4 cm) renal tumors with predominantly low signal intensity on T2-weighted images: differentiation of minimal-fat angiomyolipoma from renal cell carcinoma. AJR Am J Roentgenol 208(1):124–130. https://doi.org/10.2214/AJ R.16.16102

28. Zhang YY, Luo S, Liu Y, Xu RT (2013) Angiomyolipoma with minimal fat: differentiation from papillary renal cell carcinoma by helical CT. Clin Radiol 68(4):365–370. https://doi.org/10.1016/j.c rad.2012.08.028

29. Kim Y, Sung DJ, Sim KC, et al. (2017) Renal tumors with low signal intensities on T2-weighted MR image: radiologic-pathologic correlation. Abdom Radiol (NY) 42(8):2108–2118. https://doi.org/ 10.1007/s00261-017-1097-4

30. Yang CW, Shen SH, Chang YH, et al. (2013) Are there useful CT features to differentiate renal cell carcinoma from lipid-poor renal angiomyolipoma? AJR Am J Roentgenol 201(5):1017–1028. http s://doi.org/10.2214/AJR.12.10204

31. Wang H, Cheng L, Zhang X, et al. (2010) Renal cell carcinoma: diffusion-weighted MR imaging for subtype differentiation at 3.0 T. Radiology 257(1):135–143. https://doi.org/10.1148/radiol.10092 396

32. Hotker AM, Mazaheri Y, Wibmer A, et al. (2016) Use of DWI in the differentiation of renal cortical tumors. AJR Am J Roentgenol 206(1):100–105. https://doi.org/10.2214/AJR.14.13923

33. Yu X, Lin M, Ouyang H, Zhou C, Zhang H (2012) Application of ADC measurement in characterization of renal cell carcinomas with different pathological types and grades by 3.0T diffusion-weighted MRI. Eur J Radiol 81(11):3061–3066. https://doi.org/10. 1016/j.ejrad.2012.04.028

34. Jhaveri KS, Elmi A, Hosseini-Nik H, et al. (2015) Predictive value of chemical-shift MRI in distinguishing clear cell renal cell carcinoma from non-clear cell renal cell carcinoma and minimal-fat angiomyolipoma. AJR Am J Roentgenol 205(1):W79–86. https://d oi.org/10.2214/AJR.14.13245

35. Outwater EK, Bhatia M, Siegelman ES, Burke MA, Mitchell DG (1997) Lipid in renal clear cell carcinoma: detection on opposed-phase gradient-echo MR images. Radiology 205(1):103–107. http s://doi.org/10.1148/radiology.205.1.9314970

36. Hindman N, Ngo L, Genega EM, et al. (2012) Angiomyolipoma with minimal fat: can it be differentiated from clear cell renal cell carcinoma by using standard MR techniques? Radiology 265(2):468–477. https://doi.org/10.1148/radiol.12112087

37. Agnello F, Roy C, Bazille G, et al. (2013) Small solid renal masses: characterization by diffusion-weighted MRI at 3 T. Clin Radiol 68(6):e301–308. https://doi.org/10.1016/j.crad.2013.01.002

38. Muller MF, Prasad PV, Bimmler D, Kaiser A, Edelman RR (1994) Functional imaging of the kidney by means of measurement of the apparent diffusion coefficient. Radiology 193(3):711–715. https://d oi.org/10.1148/radiology.193.3.7972811

39. Siegel CL, Aisen AM, Ellis JH, Londy F, Chenevert TL (1995) Feasibility of MR diffusion studies in the kidney. J Magn Reson Imaging 5(5):617–620

40. Cova M, Squillaci E, Stacul F, et al. (2004) Diffusion-weighted MRI in the evaluation of renal lesions: preliminary results. Br J Radiol 77(922):851–857. https://doi.org/10.1259/bjr/26525081

41. Namimoto T, Yamashita Y, Mitsuzaki K, et al. (1999) Measurement of the apparent diffusion coefficient in diffuse renal disease by diffusion-weighted echo-planar MR imaging. J Magn Reson Imaging 9(6):832–837
42. Notohamiprodjo M, Reiser MF, Sourbron SP (2010) Diffusion and perfusion of the kidney. Eur J Radiol 76(3):337–347. https://doi.org/10.1016/j.ejrad.2010.05.033
43. Thoeny HC, De Keyzer F, Oyen RH, Peeters RR (2005) Diffusion-weighted MR imaging of kidneys in healthy volunteers and patients with parenchymal diseases: initial experience. Radiology 235(3):911–917. https://doi.org/10.1148/radiol.2353040554
44. Reuter VE, Tickoo SK (2010) Differential diagnosis of renal tumours with clear cell histology. Pathology (Phila) 42(4):374–383. https://doi.org/10.3109/00313021003785746